Chapter II

Reagents and Physico-chemical Methods

In this chapter, an outline of the materials, procedures and various physico-chemical methods employed for the synthesis and characterization of new CPs and MOFs are discussed.

2.1 Reagents

Metal salts, 1,2-benzenedicarboxylic acid (1,2-H_2bdc) and 1,2,4,5-benzene tetracarboxylicacid (H_4btec) used for the synthesis of coordination polymers and MOFs were of Merck or BDH grade. We have also employed different alkylamines as templating agents, which are also of Merck grade, and are used as received. The amines used are methylamine, ethylamine, monoethanolamine, propyl amine, butylamine, pentylamine, hexylamine, 1,2-diaminoethane, 1,2- diaminopropane, 1,3-diaminopropane, 1,4-diaminobutane, 1,2-diamino cyclohexane and 1,6-diaminohexane. The solvents used for the present study were double distilled water, Merck grade methanol or DMF and were purified by the standard procedures.[175]

2.2 Preparative details

Throughout the work, soft solution route was employed for the synthesis of amine templated, poly carboxylate derived multi-dimensional coordination polymers and MOFs with anionic frame works. Stoichiometric quantities of metal acetates and aliphatic flexible mono/diamines were mixed well with constant stirring in aqueous medium. Resulting suspension was mixed with hot aqueous/methanolic/DMF solution of benzene di/tetra carboxylic acids. The mixtures were stirred well and kept warm for about an hour. The expected metal complexes were obtained either in the soluble or solid form which were

filtered and kept at room temperature for crystallization without further disturbance. Most of the cases good quality crystals were separated out whereas others yielded crystalline powders. The product obtained were collected, washed and dried in air. Details of the steps involved in the synthesis were depicted in the respective chapters.

2.3 Physical Measurements

2.3.1 Spectral methods

2.3.1.a. Infrared spectroscopy

Infrared spectroscopy can be used to study the structural and bonding features of the complexes in the quantitative as well as qualitative aspect. It is helpful in assessing the site of coordination, nature of metal-ligand interactions and structure determination of coordination compounds. The distinction between geometrical or linkage isomers can be easily made by employing IR spectral analysis. Jahn-Teller distortion effects have also been inferred from infrared spectra. Coordination complexes mainly show ligand based vibrations, metal-ligand vibrations and also lattice vibrations. The newly formed M-L (M=metal & L=ligand) bonds consequently alters the electronic structure, the energy state and overall symmetry of the complex. These changes affect the vibrational modes of bonds in the ligand, which consequently changes the nature of vibrational spectrum also.

In the present study, we have recorded the IR spectra by using Schimadzu IR-470 spectrophotometer operating in the range 4000-400cm^{-1} using samples in the form of KBr pellets. From the IR data of the synthesized CPs and MOFs, we could mainly recognize the bands due to amine ($–NH_2$), Hydroxo(-OH), C-H and carboxylate($–COO^-$) groups.

2.3.1.b. Electronic spectra

Electronic absorption spectroscopy is a very good technique used for the structure elucidation of transition metal complexes. The electronic absorption spectrum often provides quick and consistent information about the arrangement of ligands around the metal ion. For example, octahedral complexes can easily be distinguished from tetrahedral ones on the basis of position and intensity of their absorption bands. The number of bands, their frequencies and molar absorptivities should all be considered for predicting the geometry of the metal centers. Infrared and magnetic susceptibility data should be considered along with electronic spectral measurements to aid the assignment of structures of metal complexes. It is possible to determine the point group symmetries in the coordination sphere and also assign possible coordination, geometric and linkage isomers from the electronic spectra.

A Schimadzu UV-160A spectrophotometer operating in the range 200-1100 nm was used for electronic spectral studies. Some of the spectra were taken using the aqueous solution of the sample in the range 200-1100 nm and for the insoluble solid samples; the solid-state spectra were taken in the range 200-800 nm. Another method employed for scanning the electronic spectra of insoluble solid sample was by converting it into a paste with nujol and then spreading the paste uniformly on a Whatmann filter paper strip to get a transparent dispersion of the sample. The reference used was a Whatmann filter paper strip coated with nujol and the spectral range was 200-1100 nm. For recording the spectra in solution quartz cuvettes with path length of either 1 cm or 0.5 cm were used.

2.3.1.c EPR spectroscopy

Electron paramagnetic resonance (EPR) spectroscopy is a very powerful and sensitive method for the characterization of the electronic structures of

materials with unpaired electrons. There are varieties of ESR techniques, each of them has its own advantages. In continuous wave ESR (CW-ESR), the sample is subjected to a continuous beam of microwave irradiation of fixed frequency and the magnetic field is swept. Different microwave frequencies may be used and they are denoted as S-band (3.5 GHz), X-band (9.25 GHz), K-band (20 GHz), Q-band (35 GHz) and W-band (95 GHz). EPR spectra are applicable to transition metal ions or complexes containing unpaired electrons. EPR spectrum of a complex gives two information's. First one is the structural information from hyper fine splitting and the second is the spin density information.

For the present work, the EPR spectra of Cu(II) complexes were recorded using a Varian E-112 EPR spectrophotometer operating at 9.1 GHz with a microwave power of 5mw. The field set is around 3000G and the scan range used was either 2000 or 1000 G. The spectra obtained were at LNT of 77 K. DPPH or TCNE radicals were used as `g` marker.

The basic principle of EPR is very much similar to that of NMR. Practical difference arises from the fact that the magnetic moment of an electron is substantially larger than that of the proton. The energy of resonance absorption is,

$$\Delta E = h\nu = g\beta H \qquad \text{……..2.1}$$

Where ν denotes the frequency of radiation used, h is the Planck's constant, g is the spectroscopic splitting factor, β is the Bohr magneton and H is the external magnetic field applied.

The spin Hamiltonian for the interaction of an electron with the magnetic field can be given by the equation,

$$\hat{H} = g\beta H \hat{S}_z \qquad \text{…….. 2.2}$$

Where the g value for free electron has the value 2.0023

$\beta = eh/2m_ec$, with a value of 9.273 x 10^{-21} erg $gauss^{-1}$, $\hat{S}_z$ is the spin operator and H is the applied field strength. The spectra of powder samples result from the super imposition of all the orientations of single paramagnetic centers and has a shape influenced by the anisotropic part of the Hamiltonian. The nuclear spin of copper (I=3/2) splits both the parallel and perpendicular lines in to 4 hyperfine lines. The energy absorbed during a resonance transition hν can be expressed as,

$$h\nu = g\beta H + Am_i \qquad \text{……..} \quad 2.3$$

For copper, the nuclear spin quantum number, mi takes values +/- 3/2 and +/-1/2

We have analyzed the EPR spectra of copper complexes mostly by assuming axial symmetry, for which the relevant spin Hamiltonian is,

$$\hat{H} = g_{11}\beta H_z S_z + g_\perp \beta (H_y S_y + H_x S_x) + A_{11}^M S_z I_z^M + A_\perp^M (S_y I_y^M + S_x I_y^M) + A_{11}^N S_z I_z^N$$

$$+ A_\perp^N S_z I_z^N + A_\perp^N (S_y I_y^N + S_x I_x^N) \qquad \text{...……}2.4$$

Where Z-axis is the symmetry axis of the molecule and S and I terms are components of the electron and nuclear spins in the specified directions. In equation 2.4, the first two terms are Zeeman for electron, third and fourth terms are the components due to the nuclear (metal) hyperfine interaction and fifth and sixth terms are contribution from the super hyperfine interaction of the ligand and the unpaired electron.

In a rigid medium, each molecule has an orientation with respect to the magnetic field and the tensor g and the hyperfine splitting constant A can be written as,

$$g = (g_{\|}^2 \cos^2\theta + g_\perp^2 \sin^2\theta)^{1/2} \qquad \text{……}2.5$$

$$A = \frac{(A_{11}^2 g_{11}^2 \cos^2\theta + A_{\perp}^2 g_{\perp}^2 \sin^2\theta)^{1/2}}{g} \qquad \ldots\ldots\ldots\ldots\ldots 2.6$$

$$H_{11} = \frac{h\upsilon}{g_{11}\beta} \text{ and } H_{\perp} = \frac{h\upsilon}{g_{\perp}\beta} \qquad \ldots\ldots\ldots\ldots\ldots 2.7$$

The hyperfine splitting arises because of the interaction of electron spin with its own nucleus, and further to that of the super hyperfine splitting due to the electron spin interacting with the nuclear spin of the neighboring atom(s). The parallel and perpendicular components arise because of the anisotropy of the field felt at the free electron because of the overall structure of the molecule and also the orientation of the molecule with respect to the external magnetic field applied.

The hyperfine splitting constant (A) can be calculated from the following equation,[176]

$$A = \frac{g_{11}^2 + A_{11}^2}{g_{11}^2 A_{11}^2 + g_{\perp}^2 A_{\perp}^2} \qquad \ldots\ldots\ldots\ldots 2.8$$

The average of g (g_{av}) can be calculated from the equation,

$$g_{av} = \frac{2}{3} g_{\perp} + \frac{1}{3} g_{11} \qquad \ldots\ldots\ldots\ldots .. 2.9$$

For tetragonally compressed Cu(II) complexes, $g_{\perp} > g_{\parallel}$, where g = 2 and for tetragonally elongated Cu(II) complexes $g_{\parallel} > g_{\perp} > 2$. In a square planar Cu(II) complexes, if the unpaired electron resides in the $d_{x^2-y^2}$ orbital, $g_{\parallel} > g_{\perp} > 2$ while $g_{\perp} > g_{\parallel} > 2$ when the unpaired electron in the d_{z^2} orbital. The $g_{\parallel}$ is a parameter, which depends on the nature of covalency. For a covalent complex $g_{\parallel} < 2.3$ and for an ionic environment $g_{\parallel} = 2.3$ or more. For a square planar Cu(II) complex, the g value can be calculated as,

$$g_{\perp} = 2.002 - \frac{2k_{\perp}^{2}\lambda}{\Delta Exz} \text{ and } g_{11} = 2.002 - \frac{8k_{11}^{2}\lambda}{\Delta Exy} \qquad \text{…….. 2.10}$$

Where K is the orbital reduction factor and λ is the spin orbit coupling constant. ΔE_{xz} is the energy of $^2B_{1g} \rightarrow {}^2E_g$ and ΔE_{xy} is the energy of $^2B_{1g} \rightarrow {}^2B_{2g}$. On combining the expressions in equation 2.10, we get the value of G as given below,

$$G = \frac{g_{11} - 2.002}{g_{\perp} - 2.002} = \frac{4K_{11}^{2}\Delta E_{xz}}{K_{\perp}^{2}\Delta E_{xy}} \qquad \text{……2.11}$$

Calculated value of G gives an idea about the strength of the ligand, whether strong or weak. If G < 4.0, the ligand forming Cu(II) complex is regarded as a strong field ligand. In the case of Cu(II) complexes the in plane σ covalency parameter α^2_{Cu} is related to A_{11}, g_{11} and $g_{\perp}$ according to Kivelson and Neiman equation, [177]

$$\alpha_{cu}^{2} = -(A_{\parallel}/0.036) + (g_{\parallel} - 2.002) + 3/7(g_{\perp} - 2.002) + 0.04 \qquad \text{…2.12}$$

The value of α^2_{Cu} is in between 0.5 to 0.8 for covalent bonding and for ionic the value is one. α^2_{Cu} is inversely related to the covalency of Cu-N bond. For a copper compound which has lower value for $\alpha^2_{Cu,}$ the covalency of Cu-N bond is high or the ionic character will be less. In the case of σ bonding, the ionic character increases as the ligand donor ability increases.

2.3.1.d Fluorescence spectroscopy

Mainly this spectroscopy is concerned with electronic and vibrational states. Generally, the species being examined will have a ground electronic state or a low energy state and an excited electronic state of higher energy. Each of these ground and excited electronic states comprises vibrational states also. In fluorescence spectroscopy, the species get excited from its ground state by

absorbing photons, and jumps to one of the vibrational states in the excited electronic state. Collisions with other molecules cause the excited molecule to lose vibrational energy until it reaches the lowest vibrational state of the excited electronic state. The molecule then drops down to one of the various vibrational levels of the ground electronic state again, emitting a photon in the process. As molecules may drop down into any of the vibrational levels in the ground state, the emitted photons will have different energies, and thus frequencies. Therefore, by examining the different frequencies of light emitted along with their relative intensities, the structure of the different vibrational levels can be assigned. Experimentally, the different wavelengths of fluorescent light emitted by a sample are measured using a monochromator, holding the excitation light at a constant wavelength. This is known as the emission spectrum. An excitation spectrum is the opposite, whereby the emission light is held at a constant wavelength, and the excitation light is scanned through different wavelengths (via a monochromator). During this work, we have made the photoluminescence studies on a PerkinElmer LS 45 Fluorescence Spectrometer.

2.3.2 Elemental analysis

The chemical compositions of all the complexes were evaluated by analyzing for C, H and N percentage by using Vario EL III elementar analyzer.

2.3.3 Thermal Analysis

Thermal methods of analysis may be defined as those techniques in which change in physical and /or chemical properties of a substance are measured as a function of temperature. The study of reactions involving solids has three aspects. They are phenomenological, thermodynamic and kinetic. The phenomenological study concerned with the quantitative and semi quantitative observation occurring during the reactions. The thermodynamic

aspect is static in nature. It is related to the initial, final and equilibrium states of the system and the driving force behind the transformations. The kinetic approach is mainly concerned with the rate of transformations of the reactants in to products and the mechanism of transformations. In the present work, we mainly look in to the influence of procedural factors in kinetic parameters obtained from non-isothermal kinetic analysis using TG and DTG data.

2.3.3.1 Thermogravimetry (TG)

This technique is generally employed to find out the thermal stability of CPs and MOFs. In TG analysis, the mass of a sample is recorded continuously as a function of temperature or time as the temperature of the sample is increased (usually linear with time). From the analysis, a plot of mass or mass percent as a function of time or temperature is obtained which is called thermogram or thermal decomposition curve is obtained. TG analysis also gives a quantitative measurement of any weight loss associated with transition. The changes in mass are as a result of the rupture and /or formation of chemical bonds at elevated temperatures and loss of some volatile products. TG curves are characteristic for a given compound because of unique sequence of physico-chemical reactions, which occur over definite temperature ranges. These changes are a function of its temperature dependent molecular structure. From such curves, the thermodynamics and kinetics of various chemical reaction mechanisms and get an idea of the intermediates and final products being formed.

Thermo gravimetric analysis is usually of two types.

(a) Dynamic TGA or non-isothermal method:

In this method the sample is subjected to conditions of continuous increase in temperature usually linear with time.

(b) Isothermal or static TGA

In this technique, the sample is maintained at a constant temperature for a particular period of time during which any changes in weight are noted.

2.3.3.2. DTG

In derivative thermogravimetry (DTG), the first derivative of mass change with respect to time is recorded as a function of time or temperature. The derivative curve may be obtained either from TG curve by manual differentiation methods or the electronic differentiation of the TG signals. The area of the DTG peak at any temperature gives the rate of mass change at that temperature. The DTG curve allows the ready determination of the temperature at which the rate of mass change is maximum and the initial temperature (T_i) at which cumulative mass change begins and the final temperature (T_f) at which the cumulative mass change reaches a maximum corresponding to a complete transition.

TG and DTG studies have much more importance in the case of CPs and MOFs. This may be due to the fact that on varying the temperature, the CP or MOF may be changing to another product with the removal of one or two ligand moieties. These modified high temperature compounds can have completely modified novel structures, which could be interesting. From non-isothermal studies of samples developed in the present work, the phenomenological aspects have been studied. From this aspect it is possible to find out the thermal stability of a substance the initiation temperature (T_i), the final temperature (T_f), the temperature of maximum loss (T_s), the physicochemical reactions which takes place over definite temperature ranges, the intermediates formed and the final product of the reaction.

2.3.4 Powder X ray diffraction

The powder X ray diffraction studies of some of the coordination polymers and MOFs were recorded to check their crystalline features and purity. The PXRD were recorded using Rigaku make model mini flex PXRD in the 2θ range 5-50^{o}. The diffractograms are reproduced in the concerned section.

2.3.5 Single crystal X-ray diffraction studies

Single crystal X-ray crystallography is an important technique empolyed for identifying the atomic and molecular structure of a crystal, in which the crystalline atoms cause a beam of incident X-rays to diffract into many specific directions. This diffraction consists of three-dimensional array of reflections that satisfy the conditions of Bragg's law, $n\lambda = 2d \sin\theta$. By measuring the angles and intensities of these diffracted beams, a crystallographer can produce a three-dimensional picture of the density of electrons within the crystal. From this electron density, the mean positions of the atoms in the crystal can be determined, as well as their chemical bonds, their disorder and various other information. The accurate information of the molecular geometry is becoming increasingly important in chemical and biological fields. The three dimensional atomic coordinates obtained from crystallographic studies are often the starting point for most molecular modeling, drug design and molecular orbital calculations.

In our work, various single crystal XRD instruments could be used for the structure determination and the instruments are Siemen's Smart-CCD diffractometer equipped with a normal focus, 2.4 kW sealed tube X-ray source (Mo Kα radiation, λ = 0.71073Å) operating at 40 kV and 40 mA., Bruker axs (Kappa apex2) CCD diffractometer and Enraf-Nonius CAD4 diffractometer.

2.3.6 Magnetic Susceptibility Measurements

Magnetic susceptibility is the ratio of the intensity of magnetism induced in a substance to the intensity of field to which it is subjected. Quantitative measures of the magnetic susceptibility provide insights into the structure of materials, providing insight into bonding and energy levels. Magneto-chemistry is used to investigate the magnetic properties of transition metal complexes. Magnetic moment can provide information about the oxidation state of the metal ion, possible geometry of the complex, ligand field strength, purity of the complex, and symmetry properties of the complexes. In first row transition metals, the spin only magnetic moment can be calculated using the spin only equation,

$\mu_{(s,o)} = [4S(S+1)]^{1/2}$. Diamagnetic corrections for the rest of the molecules were computed from Pascal's constants.

Gram susceptibility was calculated using the formula,

$$\chi_g = C_{bal.} \times l/(R-R_0)/ 10^9 \times m$$

C_{bal} is the calibration constant of the balance, usually set as 1. l is the sample length (in cm). m is the sample mass (in g). R is the reading obtained for tube plus sample. R_0 is the empty tube reading (normally a negative value). The effective magnetic moments, μ_{eff}, were calculated from corrected molar magnetic susceptibility, χ_m*.

$\chi_m = \chi_g^* \times$ mol.wt

$\chi_m^* = \chi_m + D$

Where D is the diamagnetic correction

$\mu_{eff} = 2.828 (\chi_m^* \times T)^{1/2}$ BM

T is the temperature of the sample.

Magnetic moments of all the complexes were measured at room temperature using the Sherwood Scientific Magnetic susceptibility Balance (M.S.B).

We have also investigated the low temperature magnetic properties of a few of the prepared complexes. Magnetic susceptibility(χ) was measured on the powder sample as a function of temperature (1.8 K $\leq$ T $\leq$ 300 K) and at different applied magnetic fields (H) using a SQUID-VSM (Quantum design). The magnetization isotherm (M vs H) was measured at T = 2.5 K in static fields up to 14 T with the VSM and in pulsed magnetic fields up to 30 T at the Dresden High Magnetic Field Laboratory (HLD).

2.3.7 Coordination chemistry of Co(II), Ni(II), Cu(II) , Zn(II) and Cd(II) systems

The context of our study was mainly based on the divalent metal ions Co(II), Ni(II), Cu(II), Zn(II) and Cd(II). Therefore it is relevant to discuss the coordination features of these metal systems.

Coordination chemistry of Co(II)

Cobalt(II) has a significant role in the development of coordination chemistry because its spectra were indicative of their stereochemistry and was very easy to prepare its complexes without special precautions. It forms octahedral and tetrahedral complexes very easily. However, a fair number of square ones as well as five coordinates are reported.[178] Co(II) forms tetrahedral complexes more readily than any other transition metal ion because of the slight stability difference between octahedral and tetrahedral Co(II) complexes, there are several cases in which the two types with the same ligand may be in equilibrium. Eg: $[Co(H_2O)_4]^{2+}$ are in equilibrium with $[Co(H_2O)_6]^{2+}$.

Tetrahedral complexes of $[CoX_4]^{2-}$ are generally formed with monodentate anionic ligands such as Cl^-, Br^-, OH^-, I^-, SCN^-, N_3^- and with a combination of two such ligands and two neutral ones (L) tetrahedral complexes of the type $[CoL_2X_2]$

are formed. Co(II) can easily form tetrahedral complexes with monodentate anions like N- alkyl salicylaldiminato and bulky β-diketonate anions also.

Co(II) forms complexes with higher coordination numbers with less hindered ligands. Eg: -bis N-methyl salicylaldiminato) cobalt (II) is a dimer with five coordinate Co(II) atoms is formed, while [Co (acac) $_2$] is a tetramer in which each cobalt atom is six coordinated as shown in Fig. 2.1.

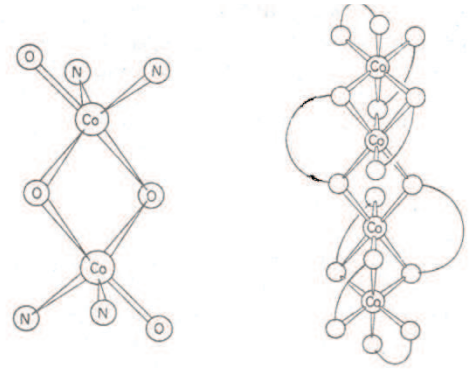

(a) (b)

Fig.2.1. *Structures of (a) the dimer of bis-N-methyl salicylaldiminato Co(II) and (b) the tetramer of bis (acetyl acetonato) Co(II)*

Planar complexes are formed with several bidentate mono anions such as dimethyl glyoximate, amino oxalate, and several neutral bidentate ligands. It also forms a number of well-defined five coordinate complexes mainly with polydentate ligands. The d^7 electronic configuration is most favoured to form the tetrahedral as opposed to the octahedral stereochemistry. Ligand polarisability as well as ligand size is the important factors with the more polarisable ligands favouring tetrahedral structures. Most O and N donors favour octahedral coordination.

Octahedral complexes are of Co(II) are pale red or purple coloured, while the tetrahedral ones are intense blue. The Co(II) in octahedral coordination has the ground state either $^4T_{1g}$ (t_{2g}^3, eg^2) or ^2E_g(t_{2g}^6,e_g^1) depending up on the strength

of ligand field. For most octahedral complexes, $^4T_{1g}$ is the ground state; only CN^- ion form low spin complexes with ground state ^2E_g.

High spin d^7 complexes show three absorption bands in an octahedral field. They are,

υ_1 $\quad ^4T_{1g} \rightarrow ^4T_{2g}$ $\quad (\sim 8000 cm^{-1})$

υ_2 $\quad ^4T_{1g} \rightarrow ^4A_{2g}$ $\quad (\sim 16000 cm^{-1})$

υ_3 $\quad ^4T_{1g} \rightarrow ^4T_{2g}(P)$ $\quad (\sim 19400 cm^{-1})$

Since the peaks are close together, it shows that this complex is close to the cross over point between $^4A_{2g}$ and $^4T_{2g}$ states on the energy level diagram. A schematic representation is shown in Fig. 2.2

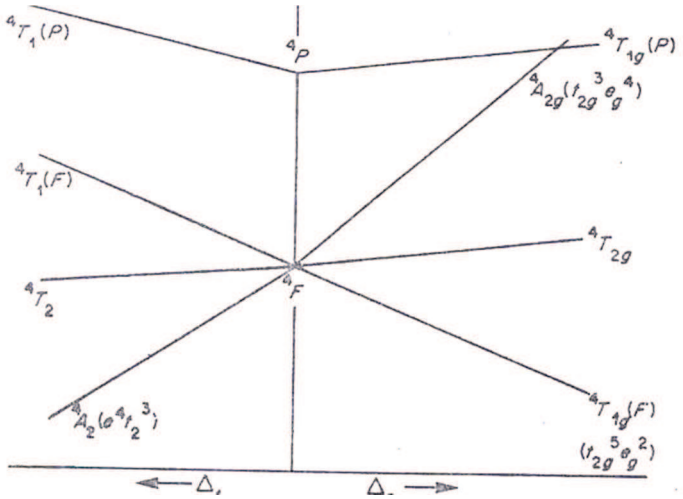

Fig.2.2 *Orgel diagram of tetrahedral and octahedral Co(II)*

$^4T_{1g} \rightarrow {}^4A_{2g}(\nu_2)$ transition is essentially a two-electron transition as the excitedstate configuration is $t_{2g}^3 e_g^4$, while the ground state is $t_{2g}^5 e_g^2$.

In the case of five coordinate Co(II) complexes, the electronic transition will be described as follows. In square pyramidal, the ground state is a quasi-degenerate state $^4A_2 + {}^4E$.

The expected electronic transition are from,[179,194,195]

$^4A_2+^4E \rightarrow {}^4B_2$ (~5000 cm^{-1})

$^4A_2+^4E \rightarrow {}^4E$ (~7000 cm^{-1})

$^4A_2+^4E \rightarrow {}^4B_1$ (~11000 cm^{-1})

$^4A_2+^4E \rightarrow {}^4E^{(p)}$ (~17000 cm^{-1})

$^4A_2+^4E \rightarrow {}^4A_2^{(p)}$ (~20000 cm^{-1})

In trigonal bipyramidal geometry, $^4A'_2$ is the ground state, the electronic transitions are,

$^4A'_2 \rightarrow {}^4A''_1 + {}^4A''_2$ (~3500 – 4000 cm^{-1})

$^4A'_2 \rightarrow {}^4E''$ (~5000 – 7000 cm^{-1})

$^4A'_2 \rightarrow {}^4E'$ (~8000 – 11000 cm^{-1})

$^4A'_2 \rightarrow {}^4A'^{(p)}_2$ (~15000 – 17000 cm^{-1})

$^4A'_2 \rightarrow {}^4E''^{(p)}$ (~20000 – 22000 cm^{-1})

The molar extinction coefficients of tbp are generally higher than square pyramidal. For both systems $^4F \rightarrow {}^4F$ transitions are less intense compared to $^4F \rightarrow {}^4P$ transition.

The ground state of tetrahedral Co(II) complexes is $^4A_2$ ($e^4t_2^3$). The three possible transitions, two of which appear in the IR and the third in the red region and is responsible for the usual blue colour of the tetrahedral Co(II) complexes. In $CoCl_4^{2-}$, two bands in the region of 5800 and 15000 cm^{-1}, corresponding to the transitions $^4A_2 \rightarrow {}^4T_1^{(F)}$ (ν_2) and $^4A_2 \rightarrow {}^4T_1^{(p)}$($\nu_3$) respectively. $^4A_2 \rightarrow {}^4T_2$ (ν_1) transition is orbitally forbidden for regular tetrahedral Co(II) although vibronically allowed. This band occurs at (~3300 cm^{-1}), which is outside the range of most UV-visible spectrophotometers and is often overlapped by ligand bands due to vibrational transitions.[179,194,195]

Coordination chemistry of Ni(II)

Ni(II) forms large number of complexes with coordination numbers ranging from four to six and the main structural types are square planar or tetrahedral (for four coordination), trigonal bipyramidal or square pyramidal (for five coordination) and octahedral (for six coordination). The maximum coordination number shown by Ni(II) ion is six. A large number of neutral ligands especially amines displace some or all the water molecules in the octahedral $[Ni(H_2O)_6]^{2+}$ ion to form complexes such as *trans*-$[Ni(H_2O)_2(NH_3)_4](NO_3)_2$, $[Ni(NH_3)_6](ClO_4)_2$, $[Ni(en)_3]SO_4$ etc. Such amine complexes have blue or purple colours in contrast to the bright green colour of the hexa aqua nickel ion. This is because shift in absorption bands when H_2O ligands are replaced by others lying towards the stronger end of the spectro-chemical series. In an octahedral Ni(II) complex the ground state configuration is $t_{2g}^6 e_g^2$ and $^3A_{2g}$ is the ground state term. The three spin allowed transitions are,[179]

$^3A_{2g} \rightarrow {}^3T_{2g}$ (~8000-13000cm^{-1})

$^3A_{2g} \rightarrow {}^3T_{1g}(F)$ (~15000-19000cm^{-1})

$^3A_{2g} \rightarrow {}^3T_{1g}(P)$ (~25000-30000cm^{-1})

The molar absorptivities of these bands are generally below 20. Some spin forbidden triplet to singlet bands may also appear. The orgel diagram for Ni(II) complexes will be shown in Fig.2.3.

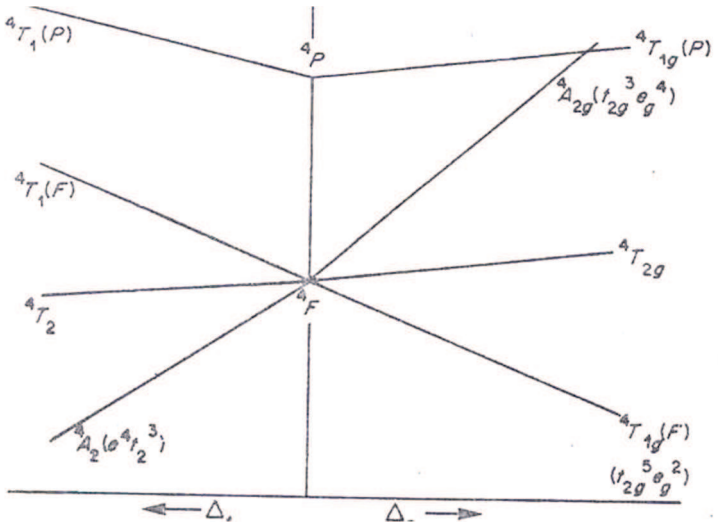

Fig 2.3 *Orgel diagram for tetrahedral and octahedral Ni(II)*

The ratio of frequencies ν_2/ν_1 of the second and first maxima lies in between 1.5 to 1.7. The octahedral Ni(II) complexes of ammonia, DMF (N, N dimethyl formamide), DMA (N, N dimethyl acetamide) are colored purple, green and yellow respectively. If all the three bands are observed, B′ for Ni(II) complexes can be calculated from the equation,

$$15\ B' = (\nu_2 + \nu_3 - 3\nu_1)$$

Tetragonally distorted octahedral Ni(II) of the type NiA_4B_2 in which the two ligands B occupy either the cis or trans positions will show a spectrum similar to octahedral complexes.[179,194] The molar absorptivities of the bands will generally be higher for tetragonally distorted octahedral complexes than for the octahedral complex. Ni(II) complexes can exist either as a diamagnetic or paramagnetic species depending up on its coordination number and geometry around the metal center. The former shows square planar coordination while the later shows octahedral coordination. Metals with d^8 configuration are particularly prone to form square planar complexes[179] (with strong field ligands), even though in such σ bonded complexes, the metal ion has an EAN of two less than that of the next inert gas. The electrostatic and steric repulsion

energies in square planar complexes are greater than in the corresponding tetrahedral complexes. The energy required to stabilize square planar complexes is provided by greater sigma and /or π bonding of the ligand to the metal.[195]

Square planar complexes of Ni(II) have typically a single band due to $^1B_{1g} \rightarrow {}^1A_{1g}$ transition at 18000-25000 cm^{-1} of intensity generally 50-100 $litremol^{-1}cm^{-1}$ and are orange yellow or red colored. A second more intense band may be observed near 23000-30000 cm^{-1} is due to charge transfer transition.

Several Ni(II) tetrahedral complexes have also been studied. Complexes of NiX_4^{2-} type were X =Cl^-, $Br^-$and I^- is of particular interest. The bands are more intense because of the lack of center of symmetry for the complex. Orbital mixing in non-centro symmetric molecules will also enhance the intensity. Electronic spectra of tetrahedral Ni(II) complexes gives the following transitions,[194]

(ν_1) $^3T_1^{(F)} \rightarrow {}^3T_2$ (~3000-5000 cm^{-1})

(ν_2) $^3T_1^{(F)} \rightarrow {}^3A_2$ (~6500-9000 cm^{-1})

(ν_3) $^3T_1^{(F)} \rightarrow {}^3T^{1(P)}$ (~12000-17000 cm^{-1})

ν_3 transition occurs in the visible and ν_2 transition in the near infrared region. Ni(II) forms numerous five coordinated complexes and the structures are trigonal bipyramidal and square pyramidal.[180] Energy level scheme for six and five membered Ni(II) complexes are as shown in Fig.2.4

In square pyramidal geometry, the expected d-d transitions are,

$^3B_1 \rightarrow {}^3E^{(P)}$ (~12000 cm^{-1})

$^3B_1 \rightarrow {}^3A_2^{(P)}$ (~19000 cm^{-1})

$^3B_1 \rightarrow {}^3E^{(P)}$ (~23000 cm^{-1})

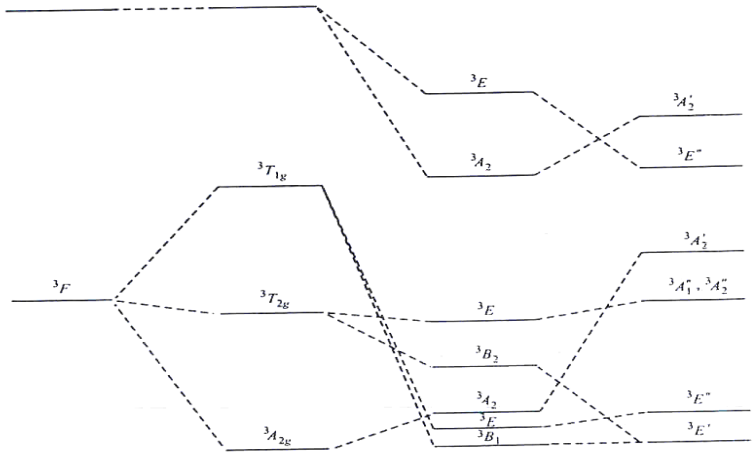

Fig 2.4 *Energy level scheme for triplet states in five coordinated Ni(II)*

A broad shoulder observed around 9000 cm^{-1} in a few cases ascribed due to transitions to $^3A_2$ and $^2B_2{}^{(F)}$.

Trigonal bipyramidal complexes of both D_{3h} and C_{3v} are known. For D_{3h} symmetry, three bands are observed.[194] They are,

$^3E_1 \rightarrow {}^3A_1'' + {}^3A_2''$ (~12000-13500 cm^{-1})

$^3E_1 \rightarrow {}^3A_2'$ (~14000-16500 cm^{-1})

$^3E_1 \rightarrow {}^3E''^{(P)}$ (~20000-23000 cm^{-1})

For C_{3v} symmetry, the bands are,

$^3E \rightarrow {}^3A_2{}^{(F)}$ (~12000 cm^{-1})

$^3E \rightarrow {}^3A_1{}^{(F)}$ (~13500 cm^{-1})

$^3E \rightarrow {}^3A_2{}^{(F)}$ (~15000 cm^{-1})

The band corresponding to $^3E \rightarrow {}^3E^{(F)}$ is observed in the near infrared region and the transition $^3E \rightarrow {}^3A_2{}^{(P)}$ in the visible region.

Coordination chemistry of Cu(II)

The dipositive state is most common for copper. The d^9 configuration makes Cu(II) subject to Jahn –Teller distortion if placed in an environment of cubic (regular octahedral or tetrahedral) symmetry and this has a profound effect in all its stereochemistry. With a few exceptions it is never observed in these regular environments. When six coordinate, the octahedron is severely distorted and the typical distortion is an elongation along one four fold axis, so that there is a planar array of four short Cu – L bonds and two trans long ones. In the limit the elongation leads to a situation indistinguishable from square coordination as found in CuO and many discrete complexes of Cu(II). Thus tetragonally distorted octahedral coordination and square coordination cannot be sharply differentiated.

For a d^9 complex in an octahedral field, the ground state is $t_{2g}^6\ e_g^3$ and is doubly degenerate while the excited state $t_{2g}^5 e_g^4$ is triply degenerate. Therefore, the transition $^2E_g \rightarrow {}^2T_{2g}$ causes the motion of a positive hole from the e_g level in the ground state to the t_{2g} level in the excited state. The ^2E_g state is highly susceptible to Jahn-Teller distortion. Therefore no regular octahedral Cu(II) complexes should exist. Great majority of Cu(II) complexes are blue or green colored. Some of these complexes may be red or brown and this is generally caused by a strong absorption in the UV region arising from the CT. These transitions tail off in to the blue end of the visible spectrum.

Cu(II) complexes are known in wide variety of structures. A very broad band with peak maximum near 15000 cm^{-1} is observed for most geometries[181]. Thus the electronic spectrum of Cu(II) is often of little value in the structural assignment. Tetragonal distortion is usually assumed to be the most common example of Cu(II) coordination.

In a tetragonal field the transitions expected are,[195]

$^2B_{1g} \rightarrow {}^2A_{1g}$ (~12000-17000 cm^{-1})

$^2B_{1g} \rightarrow {}^2B_{2g}$ (~ 15500-18000 cm^{-1})

$^2B_{1g} \rightarrow {}^2E_g$ (~17000-20000 cm^{-1})

The approximate positions of the ^2E_g and $^2B_{2g}$ states can be estimated from the g factors obtained from EPR spectra. The spectra of copper complexes are very difficult to assign even with relatively simple ligands because of the breadth of the absorption bands even at low temperature. When the ligand field is weak, the splitting is small and hence three bands are nearly superimposed to produce a broad and unsymmetric absorption band. The electronic spectrum of tetrahedral complexes of Cu(II) should be exactly similar to that for octahedral with 10 Dq value decreased by a factor 4/9. Regular tetrahedral Cu(II) complexes are uncommon. The distorted tetrahedral Cu(II) complexes show only two allowed transitions, $^2B_2 \rightarrow {}^2A_1$ and $^2B_2 \rightarrow {}^2E$. The forbidden transition $^2B_2 \rightarrow {}^2B_1$ appears as a very weak band through the combined effects of spin-orbit interaction and the low symmetry components of the Cs symmetry in the crystal. It gets its intensity by mixing with one component of the ^2E state.

For square pyramidal Cu(II) complexes, the bands are observed in the region 9000-10000 cm^{-1}, 11500-16000 cm^{-1} and 15000-19000 cm^{-1} have been attributed to the transitions $^2B_1 \rightarrow {}^2A_1$, $^2B_1 \rightarrow {}^2B_2$ and $^2B_1 \rightarrow {}^2E$ respectively. In trigonal bipyramidal complexes of D_{3h} symmetry, the absorption bands in the range 10000-11000 cm^{-1}, 12000-15500 cm^{-1} have been attributed to $^2A_1` \rightarrow {}^2E`$ and $^2A_1` \rightarrow {}^2E"$ respectively.

The ESR spectra of the complexes of tbp symmetry show typically $g_\perp > g_\parallel$ and for square pyramidal geometry complexes show $g_\parallel > g_\perp$. Fig.2.5 represents the combined orgel diagram of O_h and T_d Cu(II) complexes.

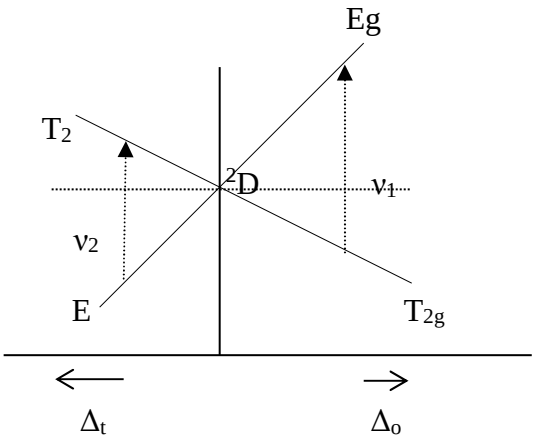

Fig. 2.5 *Orgel diagram for tetrahedral and octahedral Cu(II) complexes*

Coordination Chemistry of Zn(II) and Cd(II)

The element Zinc has a filled (n-1)*d* shell plus two n*s* electrons. The Zn^{2+} ions with their d^{10} configuration show no stereo chemical preferences arising from ligand field stabilization effects. Therefore they display a variety of coordination numbers and geometries based on the interplay of electrostatic forces, covalence and size factor. The coordination numbers 4, 5 and 6 are the common ones for zinc. Zinc forms numerous water soluble salts, for example, the nitrates, sulphates, sulphites, perchlorates and acetates that contain the aqua ions, $[M(H_2O)_6]^{2+}$. These aqua ions are also present in aqueous solutions.

The anhydrous oxide, ZnO is formed on the pyrolysis of the nitrate or carbonate or by roasting the metal in air. ZnO tend to have lattice defects leading to coloration. With Zn^{2+} the cyanide ion has a marked tendency to form linear bridges, represented as M-C≡N-M. Zinc also forms complexes with chalcogen and amine ligands. The discovery of organozinc compounds by Frankland in 1849 is of great historical importance because these were the first organometallic compounds. For zinc there are two major classes of organometallic compounds, R_2Zn and RZnX.

Zinc has marked ability to form covalent bonds to transition metals. For many of these compounds the method of preparation is to react an MX_2 compound

with a hydrido complex or a transition metal carbonylate anion, as in the following reaction.

$$2\ CpFe(CO_2)Na + ZnCl_2 \rightarrow [CpFe(CO_2)]Zn + NaCl$$

Zinc is one of the preeminently important metals in life processes, along with iron and copper. Zn and Cd follow Cu, Ag and Au and have two electrons outside filled d shells. Whereas in Cu, Ag and Au the filled shell may readily lose one or two d electrons to give ions or complexes in the II and III oxidation states this does not occur for Zn and Cd. These elements form no compounds in which the d shell is other than full. The almost invariable oxidation state of these elements is +2 and salts of most anions are known. Oxo salts are almost isomorphous with those of Mg(II) but with lower thermal stabilities. The carbonates, nitrates and sulphates all decompose to the oxides on heating. Salts such as perchlorates, nitrates and sulphates are very soluble in water and form more than one hydrate. $[Zn(H_2O)_6]^{2+}$ is probably the predominant aquo species in solutions of Zn(II) salts. The coordination chemistry of Zn(II) and Cd(II), although much less extensive than for other transition metals, is still appreciable. Tetrahedral complexes are the most common type and are formed with a variety of O-donor ligands (more readily with Zn(II) than Cd(II)), more stable ones with N-donor ligands such as NH_3, amines and CN^-. Complexes of higher coordination number can be isolated by increasing the ligand concentration or by adding large counter ions, for example, $[M(NH_3)_6]^{2+}$, $[M(en)_3]^{2+}$ and $[M(bipy)_3]^{2+}$. Complexes with SCN^- throw light on the relative affinities of the two metals for N and S-donors. In $[Zn(NCS)_4]^{2-}$ the ligand is N-bonded whereas in $[Cd(NCS)_4]^{2-}$ it is S-bonded. SCN can also act as a bridging group as in $[Cd\{S=C(NHCH_2)_2\}_2(SCN)_2]$ when linear chains of octahedrally coordinated Cd(II) are formed. With Zn^{2+} the cyanide ion has a marked tendency to form linear bridges.[182] Since there is no ligand field stabilization effect in Zn^{2+} and Cd^{2+} ions, because of their completed d shells, their stereochemistry is determined solely by considerations of size, electrostatic forces and covalent bonding forces.